Performance Comparison of PV Inverter Systems Considering System Voltage Ratings and Installation Sites

He, Jinkui; Sangwongwanich, Ariya; Yang, Yongheng; Iannuzzo, Francesco

Published in:
2021 IEEE Applied Power Electronics Conference and Exposition (APEC)

DOI (link to publication from Publisher):
10.1109/APEC42165.2021.9487456

Publication date:
2021

Document Version
Accepted author manuscript, peer reviewed version

Performance Comparison of PV Inverter Systems Considering System Voltage Ratings and Installation Sites

Jinkui He*, Ariya Sangwongwanich*, Yongheng Yang**, and Francesco Iannuzzo*
*Department of Energy Technology, Aalborg University, Pontoppidanstraede 111, Aalborg East 9220, Denmark
**College of Electrical Engineering, Zhejiang University, Zheda Rd. 38, Hangzhou 310027, China
Email: jhe@et.aau.dk, ars@et.aau.dk, yang_yh@zju.edu.cn, fia@et.aau.dk

***Abstract*—Currently, string photovoltaic (PV) inverters with wide DC and AC operating voltage ranges are available on the market, which can be employed for interfacing either 1000-V or 1500-V PV strings with different AC grid voltage levels (e.g., 400 V or 690 V). The selection of both the DC- and AC-side voltage levels should be carefully considered during the design phase. In this context, this paper compares the performance of PV systems using centralized string inverter solutions. The comparison is carried out by evaluating the power losses on each component (e.g., DC wire, inverter, AC filter, and transformer) of a 1.8-MW PV system considering different system voltage ratings and installation sites (mission profiles in Denmark and Sacramento, California). The evaluation results reveal that the impact of system voltage ratings on the energy yield of the PV system varies with mission profiles. Higher DC and AC voltage ratings can contribute to considerable energy loss reduction in both cases. However, in the cold climate, e.g., Denmark, the energy yield is more sensitive to the DC-bus voltage range, where the 1500-V PV system tied to a lower AC grid voltage (e.g., 400 V) can achieve higher energy yield.**

***Index Terms*—Photovoltaic (PV) inverters, multi-level inverters, mission profile, power loss.**

I. Introduction

String photovoltaic (PV) inverters have become an increasingly popular alternative over central inverters for multi-megawatt (MW) PV plants [1], [2]. Also, their layout can be decentralized or centralized with respect to the PV strings [3]. For the centralized solution, the string PV inverters are all placed near the low-frequency transformer, which results in the requirement of longer DC wires compared to the decentralized solution. On the other hand, the maximum DC voltage of PV strings can be increased with more PV panels connected in series, e.g., from 1000 V to 1500 V, to reduce the ohmic losses (e.g., due to lower DC current) and overall costs (e.g., due to less cabling) [4]. Currently, several string inverters with the maximum 1500-V DC voltage rating are available on the market, which can be used for interfacing either 1000-V or 1500-V PV systems with different AC grid voltage levels (e.g., 400 V, 690 V) [5], [6].

The benefits of the 1500-V PV technology over the 1000-V one have been proved by many studies [7]–[12]. Applying the 1500-V PV strings offers opportunities to reduce the installation cost (less cabling and combiner boxes), which is associated with the decrease of current ratings in different installation points [7]–[9]. Authors of [10] have explained that an extension of the DC-bus voltage range can be achieved in the case of 1500-V single-stage PV systems. In [11], the impact of different DC voltages on the PV inverter performance is presented, where the 1500-V and 2000-V PV inverters show better performance in efficiency and power density when compared with the 1000-V PV inverter. The work in [12] compares the energy harvesting for different DC and AC voltage levels and converter architectures (i.e., single-stage and two-stage), which mainly focuses on the energy losses in the PV converters. However, none of the previous studies have analyzed the impact of different DC and AC voltage ratings and installation sites on the system performance. To design a utility-scale PV system with centralized string inverters, one of the key considerations is the selection of the DC- and AC-side voltage levels, which will affect the system efficiency, energy production, and cost.

With the above, this paper compares the performance of the centralized PV string inverter solutions considering different system parameters and installation sites. The comparison is carried out through a 1.8-MW case study, where the impact of the DC- and AC-voltage ratings selection and mission profiles on the efficiency and the energy yield of the PV system is analyzed. A cold climate (Denmark) and a hot climate (Sacramento) have been used in the evaluation. The evaluation results indicate that a higher string DC voltage (e.g., 1500 V) can benefit the PV system in terms of increasing energy yield and reducing cost. However, in order to achieve higher energy yield, the selection of the AC voltage rating should be based on the mission profile characteristics of the installation site.

The rest of the paper is organized as follows. In Section II, the modeling of the centralized PV string inverter system is presented in details. After that, the procedures for analyzing the system power losses are provided in Section III, along with a case study considering three configurations (i.e., different system voltage ratings) for two installation sites (Denmark and Sacramento). Finally, Section IV gives the concluding remarks.

II. System Modeling

The model for comparing the energy loss (and yield) under different system voltage ratings and installation sites needs to

TABLE I
PARAMERTERS OF THE JKM380M-72-V PV PANEL AT THE STANDARD TEST CONDITION [15].

Parameter	Value
Maximum power P_{max}	380 W
Maximum power voltage V_{mp}	40.5 V
Maximum power current I_{mp}	9.39 A
Open-circuit voltage V_{oc}	48.9 V
Short-circuit current I_{sc}	9.75 A
Temperature coefficient of V_{oc}	-0.37 %/°C
Temperature coefficient of I_{sc}	0.048 %/°C

be developed, as shown in Fig. 1. A description of each model is given in the following.

A. Mission Profile, PV Panel, and DC Wires

In order to analyze the impact of installation sites on the PV inverter performance, two mission profiles in Denmark (cold climate) and Sacramento (hot climate) are used in this study, which consist of one-year measurements of ambient temperature and solar irradiance with the sampling rate being 1 minute/sample, as it is shown in Fig. 2 [13], [14]. Both the solar irradiance and ambient temperature in Denmark have a strong seasonal variation. In contrast, the average solar irradiance in Sacramento is relatively high throughout the year compared to that in Denmark.

A 380-W PV panel with a 1500-V DC maximum system voltage, i.e., JKM380M-72-V [15], is employed to assemble the PV arrays in this study, where a number of the PV panels are connected in series and parallel to achieve certain DC voltages and power ratings. The panel characteristic under the standard test condition (STC) is given in Table I. By applying the ambient temperature and solar irradiance of the mission profile to a proper PV panel model [16], the output voltage and current of the PV strings (corresponding to the operating point during the maximum power point tracking (MPPT) operation) can be determined and used as input parameters of the inverter model in Fig. 1.

As for the DC wire, according to the National Electrical Code (NEC) [17], the ampacity of the DC wires should be 1.25 times the short-circuit current of the PV system. Regarding the length of the DC wires, the average DC wire length for each string inverter is estimated based on the capacity of the PV plant as discussed in [3]. Then, the ohmic loss on the DC wires can be estimated as

$$P_{\text{wire}} = 2I_{\text{PV}}^2 R_{\text{wire}} \tag{1}$$

where I_{PV} is the total current of the paralleled PV strings and R_{wire} is the resistance per wire.

B. String Inverter

Generally, the power rating of string inverters with a maximum DC input voltage of 1500 V ranges from 10 kW to over 100 kW. In this case, depending on the AC grid voltage level, different number of string inverters are employed to reach the capacity for a certain PV system. Table II presents the specifications of the considered string inverter, which is a three-level I-type inverter equipped with 1200-V/150-A IGBT modules from Semikron [18]. Correspondingly, the size of the heatsink is designed to guarantee the maximum junction temperature below 125 °C under the rated operating condition and the ambient temperature being 50 °C. The inverter losses are estimated from the sum of the conduction losses and switching losses of the power semiconductor devices, which can be obtained through simulations in PLECS under a certain operating condition with the detailed loss data of the selected power module [19].

The conduction losses of power devices (e.g., IGBT or diode) can be modeled based on the forward voltage drop v_{CE} during conduction [20], [21], which can be expressed as

$$v_{\text{CE}} = V_{\text{CE0}} + \frac{V_{\text{CEN}} - V_{\text{CE0}}}{I_{\text{CN}}} i_{\text{C}} \tag{2}$$

in which V_{CE0} is the initial voltage drop, V_{CEN} represents the voltage drop at the rated current I_{CN}, and i_{C} is the collector current. After that, within one fundamental cycle, the average conduction losses can be calculated by integrating the product of the forward voltage drop and device current as [22]

$$P_{\text{con}} = \frac{1}{T_0} \cdot \int_0^{T_0} v_{\text{CE}}(t) \cdot i_{\text{C}}(t) dt \tag{3}$$

where P_{con} is the average conduction losses and T_0 is the fundamental cycle period (e.g., 20 ms for the 50-Hz AC grid).

The switching losses of power devices can be calculated from the sum of the turn-on E_{on} and turn-off energy E_{off}

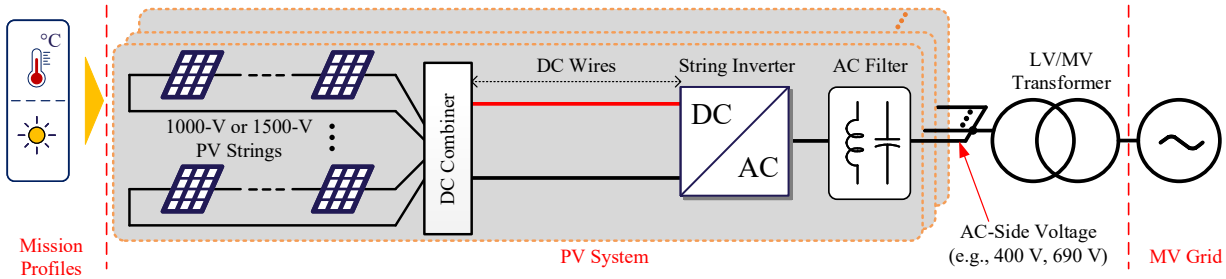

Fig. 1. System diagram of the centralized PV string inverter solution (LV: low voltage, MV: medium voltage).

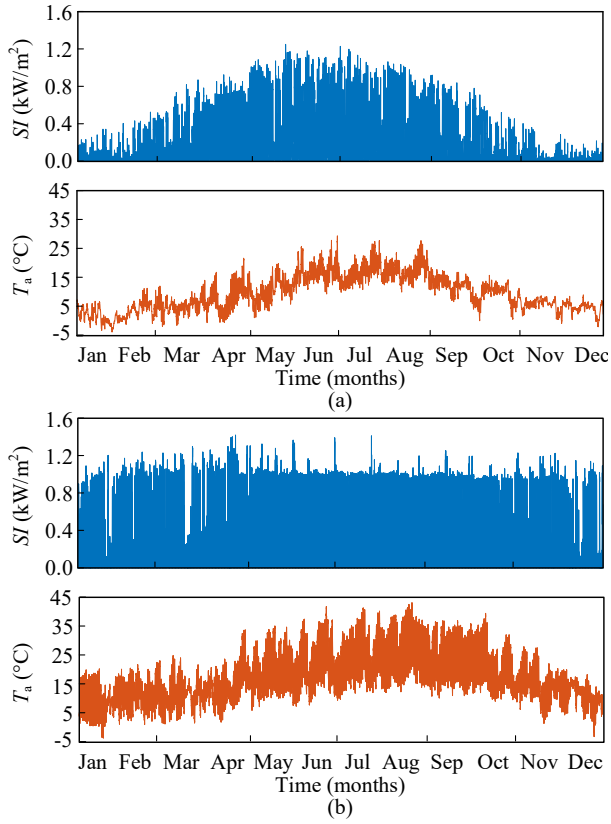

Fig. 2. One-year mission profiles (i.e., solar irradiance SI and ambient temperature T_{a}) recorded in: (a) Denmark and (b) Sacramento.

during switching. The switching energy E_{sw} of a power device can be obtained either through experimental tests (e.g., double pulse test), or the module datasheet, which is regarded as a reference of switching energy under specific gate driving parameters and junction temperatures. Based on this reference, the switching energy E_{sw} during operation can be modeled as

$$E_{\text{sw}} = E_{\text{sw(ref)}} \left(\frac{i_{\text{C}}}{I_{\text{C(ref)}}} \right)^{k_i} \left(\frac{v_{\text{CC}}}{V_{\text{CC(ref)}}} \right)^{k_v} \tag{4}$$

in which $E_{\text{sw(ref)}}$ is the switching energy reference value, $V_{\text{CC(ref)}}$ and $I_{\text{C(ref)}}$ are the test conditions for the switching loss measurement (i.e., the collector-emitter supply voltage and the collect current, respectively), v_{CC} is the actual collector-emitter supply voltage that is being applied, k_v and k_i are the exponents for the voltage and current dependency of switching losses, respectively. The values of k_v and k_i for the selected modules are summarized in Table III [21]. The average instantaneous switching loss can then be expressed as [21]

$$P_{\text{sw}} = f_{\text{sw}} \cdot E_{\text{sw(ref)}} \left(\frac{i_{\text{C}}}{I_{\text{C(ref)}}} \right)^{k_i} \left(\frac{v_{\text{CC}}}{V_{\text{CC(ref)}}} \right)^{k_v} \tag{5}$$

with P_{sw} denoting the average instantaneous switching loss and f_{sw} representing the switching frequency.

With the aforementioned loss model, the efficiencies of the PV inverter with different PV panel configurations can be obtained, as shown in Fig. 3, which can be used for long-term simulations in the form of look-up tables [23]. It is worth to note in Fig. 3 that, the efficiency of the 1500-V configuration is slightly lower than that of the 1000-V one, which can be regarded as a disadvantage of the 1500-V PV solution, namely, increased loading stress to the PV inverter.

TABLE II
PV INVERTER SPECIFICATIONS.

Parameter	Value
Rated output power P_{n} [kW]	60 / 72 / 90 / 100
Rated output current I_{n}	87 A
Rated output line-line voltage V_{LL} (RMS) [V]	400 / 480 / 600 / 690
Grid frequency f_{g}	50 Hz
Power factor $\cos(\varphi)$	1.0
Maximum DC input voltage	1500 V
DC-link voltage range for rated power	$1.44 \times V_{\text{LL}}$ to 1300 V
Switching frequency f_{sw}	6 kHz
Power module type	SkiiP 39MLI12T4V1
Heatsink thermal impedance $R_{\text{th(s-a)}}$	0.04 K/W

[1] RMS: Root-Mean-Square.

TABLE III
PARAMETERS OF THE VOLTAGE AND CURRENT DEPENDENCY OF SWITCHING LOSSES [21].

Parameter	IGBT	Diode
k_v	1.4	0.6
k_i	1.0	0.6

C. AC Filter and Transformer

Each string inverter is equipped with an LCL filter to suppress harmonics and comply with power quality requirements. The outputs of the LCL filters are connected to the low-voltage (LV) side of an isolation transformer, which steps up the AC inverter output voltage to the medium-voltage (MV) level for utility network connection. Regarding the power losses within the AC filter and the LV/MV transformer, both can be divided into copper losses and core losses. The relatively small core losses for the inductance of the AC filter are negligible, while the copper losses P_{copper} and transformer core losses P_{core} can be estimated as [24]

$$P_{\text{copper}} = 3R_{f/w}I_{f/w}^2 \tag{6}$$

$$P_{\text{core}} = 3V_{\text{MV}}^2/R_p \tag{7}$$

where $R_{f/w}$ is the resistance of the filter inductor or transformer windings, $I_{f/w}$ is the inductor or winding current, R_p is the resistance for modeling the core losses, and V_{MV} is the phase voltage of the MV side.

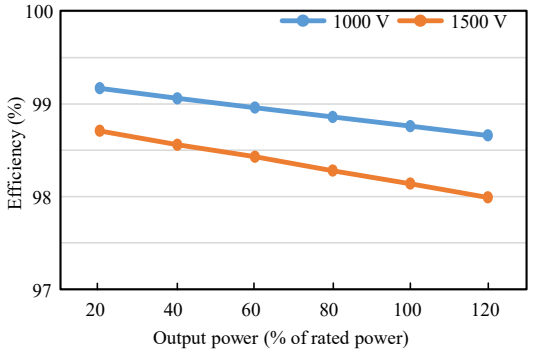

Fig. 3. Comparison of the inverter efficiency with different PV panel configurations (i.e., 1000-V and 1500-V) and the ambient temperature T_a being 25 °C.

III. Case Study

In this paper, the PV system with the rated power of 1.8 MW is considered. Accordingly, three centralized string inverter solutions are designed for the considered installation sites. Table IV summarizes the parameter of different solutions in terms of PV panel configuration, AC grid voltage, DC wire size, and inverter quantity. It is noted that different DC wire sizes and quantity of employed inverters are required for the various PV string and AC grid voltage levels, which will affect the loss and cost of the entire system. The procedure of the loss analysis is illustrated in Fig. 4. First, the output power and voltage of the PV strings can be obtained from the solar irradiance and ambient temperature profiles by using the PV panel model (e.g., look-up tables). Then, the ohmic loss in the DC wires can be calculated based on the output DC currents of the PV strings. Similarly, the power device loss and filter loss are simulated under a certain set of operating parameters and ambient temperatures to obtain look-up tables for long-term loss analysis [25]. Finally, the available PV energy, the energy loss of each part, and the system energy yield can be estimated, following the diagram shown in Fig. 4.

The total DC wire power losses and the total inverter power losses under the considered mission profiles are compared in Fig. 5, while the corresponding one-year energy losses are shown in Fig. 6. Compared with the 1000-V PV string solution, adopting 1500-V strings can reduce the DC wire energy losses to a large extent, especially when a higher AC voltage, e.g., 690 V, is adopted. The 1500-VDC 690-VAC solution also achieves the lowest inverter losses, as shown in Figs. 5 and 6. It can be noted in Fig. 6 that the main reason behind this is the lowest required number of inverters for the 1500-VDC 690-VAC solution since its energy loss per inverter is larger than that of the other two solutions. Regarding the filter and transformer losses, the considered solutions have similar energy losses, as shown in Fig. 6. Nevertheless, it is clear from the results that for both the mission profiles, the 1500-V solutions are better than the 1000-V solution in terms of the energy yield and the required number of inverters.

From the perspective of energy production, on one hand, different DC-/AC- voltage ratings mean different DC-bus

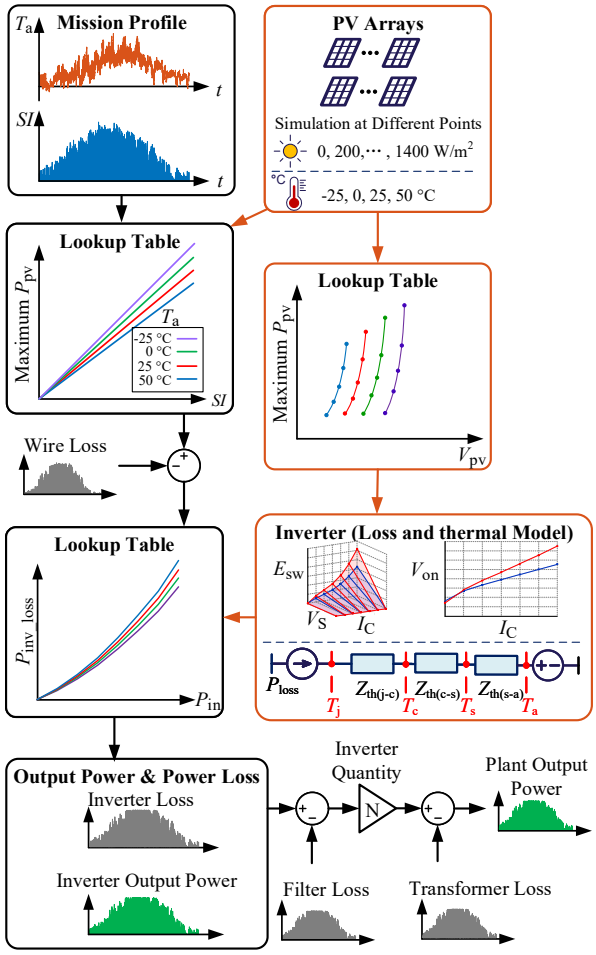

Fig. 4. Block diagram of the power loss analysis: T_a – ambient temperature, SI – solar irradiance, P_{pv} – PV output power, P_{inv_loss} – inverter loss, P_{in} – input power, T_j, T_c, T_s – junction, case, and heatsink temperature, E_{sw} – switching loss, V_{on} – voltage drop, V_s – DC-bus voltage, I_c – collect current.

voltage ranges [10], which can affect the total amount of PV energy yield. Fig. 7 shows the DC-bus voltage ranges of the considered solutions, where the 1500-VDC 400-VAC solution has a much wider operation range than the other solutions. On the other hand, the considered solutions have various energy losses under different mission profiles. For the 1.8-MW case study, the 1500-VDC 690-VAC solution achieves the highest energy production under the Sacramento mission profile. However, it has the lowest energy production under the Denmark mission profile, where the 1500-VDC 400-VAC solution (high DC-bus voltage range) is preferred for high energy yield, as shown in Fig. 5.

Overall, compared with the 1000-V configuration, although the 1500-V solutions have negative effect on the power losses of every single inverter, they can achieve lower system losses due to the considerably reduced wire losses and the number of inverters. On the other hand, a high AC voltage rating may not be the best choice for the installation sites with a cold climate, where a higher MPPT operation range will contribute to higher energy yield.

TABLE IV
CENTRALIZED STRING INVERTER SOLUTIONS.

PV Panel Configuration 1: 1000-V PV (N_s = 18, N_p = 9)	
DC wire size	2 AWG
Grid voltage	400 V
Inverter quantity	30
PV Panel Configuration 2: 1500-V PV (N_s = 27, N_p = 6)	
DC wire size	4 AWG
Grid voltage	400 V
Inverter quantity	30
PV Panel Configuration 3: 1500-V PV (N_s = 27, N_p = 10)	
DC wire size	1 AWG
Grid voltage	690 V
Inverter quantity	18
Wire length, AC filter and transformer	
Average DC wire length	200 m
AC filter	R_f = 0.008 p.u. L_f = 0.1 p.u.
Transformer	R_w = 0.005 p.u. L_w = 0.1 p.u.
	R_p = 750 p.u.

[1] N_s: Number in series

[2] N_s: Number in parallel

IV. CONCLUSION

In this paper, the centralized string inverter solution for MW-level PV plants was compared under various system voltage ratings. The comparison is based on power loss analysis of the PV plant key components (DC wire, PV inverter, AC filter, and transformer) considering two different mission profile cases (i.e., cold and hot climates). The results reveal that the 1500-V PV string inverter solution along with a higher grid voltage (e.g., 690 V) outperforms the 1000-V PV string inverter solution in terms of energy loss reduction and cost saving in the DC wires and PV inverters, especially under the Sacramento mission profile (hot climate). For the Denmark mission profile (cold climate), the solution with a higher DC-bus voltage range (e.g., 1500-V PV string and 400-V grid voltage) may be more suitable due to its higher energy yield. It should be noted that the cost of PV energy is also associated with the reliability performance of the PV inverters, which can be affected by the DC and AC voltage ratings. Careful considerations in the design and control of PV inverters are thus required to reduce the the Levelized Cost of Energy (LCOE).

ACKNOWLEDGMENT

This work has been carried out under the APETT Project, funded by the Danish Innovation Foundation, 2017-2021.

REFERENCES

[1] A. Sangwongwanich, Y. Yang, F. Blaabjerg, and D. Sera, "Delta power control strategy for multistring grid-connected PV inverters," *IEEE Trans. Ind. Appl.*, vol. 53, no. 4, pp. 3862–3870, 2017.

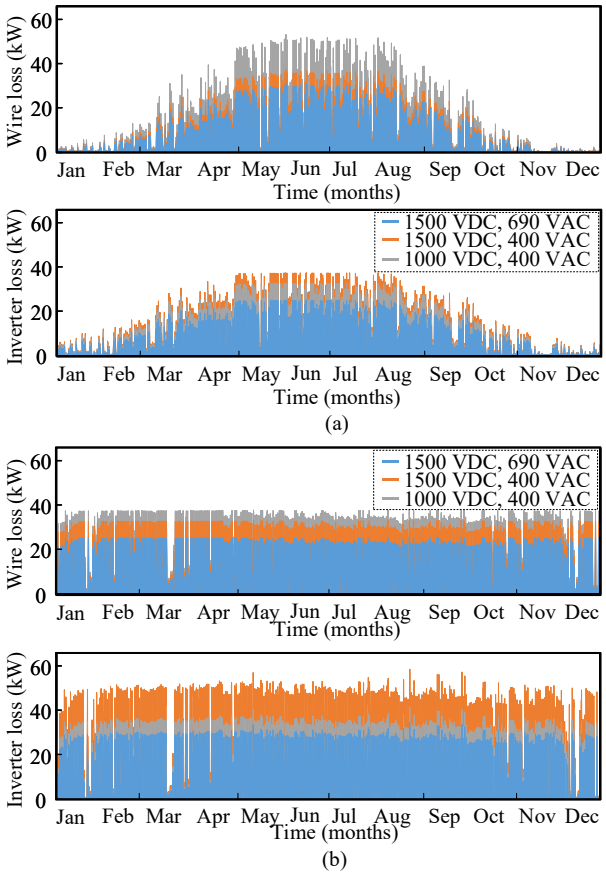

Fig. 5. Power loss of DC wires and PV inverters with different system configurations for the installation site in: (a) Denmark and (b) Sacramento.

[2] Novergy Solar. Solar String inverters are better for utility-scale solar plants and industrial solar projects. (2020). [Online]. Available: https://www.https://www.novergysolar.com/solar-string-inverters-better-utility-scale-solar-plants-industrial-solar-projects/

[3] Solar Power World. Webinar: Distributed vs. virtual ventral string. Application matters. (2021). [Online]. Available: https://www.solarpowerworldonline.com/2018/04/webinar-distributed-vs-virtual-central-string-application-matters/

[4] B. Stevanović, D. Serrano, M. Vasić, P. Alou, J. A. Oliver, and J. A. Cobos, "Highly efficient, full ZVS, hybrid, multilevel DC/DC topology for two-stage grid-connected 1500-V PV system with employed 900-V SiC devices," *IEEE J. Emerg. Sel. Top. Power Electron.*, vol. 7, no. 2, pp. 811–832, Jun. 2019.

[5] Schneider. CL125 string inverter. (2021). [Online]. Available: https://solar.schneider-electric.com/solution/string-inverter-solution-1500v/

[6] Ingeteam. 160TL photovoltaic inverter. (2021). [Online]. Available: https://www.ingeteam.com/en-us/sectors/photovoltaic-energy/p15_24_625_450/ingecon-sun-160tl.aspx

[7] E. Gkoutioudi, P. Bakas, and A. Marinopoulos, "Comparison of PV systems with maximum DC voltage 1000V and 1500V," in *Proc. IEEE PVSC*, pp. 2873–2878, 2013.

[8] R. Inzunza, R. Okuyama, T. Tanaka, and M. Kinoshita, "Development of a 1500Vdc photovoltaic inverter for utility-scale PV power plants," in *Proc. IFEEC*, pp. 1–4, Nov 2015.

[9] Z. Čorba, B. Popadić, V. Katić, B. Dumnić, and D. Milićević, "Future of high power PV plants — 1500V inverters," in *Proc. SPE*, pp. 1–5, 2017.

[10] E. Serban, M. Ordonez, and C. Pondiche, "DC-bus voltage range extension in 1500 V photovoltaic inverters," *IEEE J. Emerg. Sel. Top. Power Electron.*, vol. 3, no. 4, pp. 901–917, Dec. 2015.

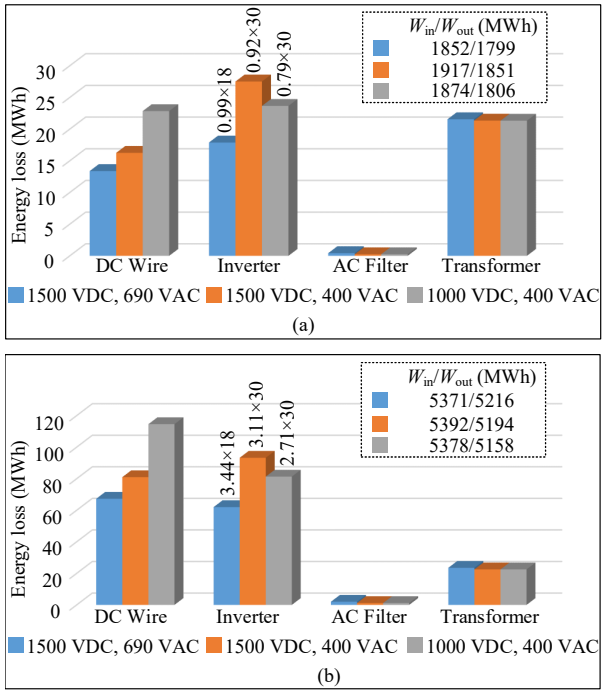

Fig. 6. One-year energy loss and yield with different system configurations for the installation site in: (a) Denmark and (b) Sacramento (W_{in}: available PV energy, W_{out}: Energy yield).

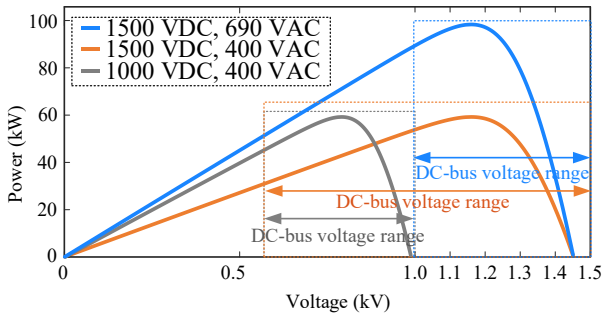

Fig. 7. DC-bus voltage range of different system configurations.

[11] C. Yan and D. Xu, "Design study of MW photovoltaic inverter," in *Proc. IEEE PEAC*, pp. 1–6, 2018.

[12] B. Stevanović, E. Serban, M. Vasić, M. Ordonez, S. Cóbreces, and P. Alou, "Energy harvesting comparison and analysis in 1000V and 1500V grid-connected PV systems," in *Proc. IEEE ECCE*, pp. 116–123, 2020.

[13] Y. Yang, A. Sangwongwanich, and F. Blaabjerg, "Design for reliability of power electronics for grid-connected photovoltaic systems," *CPSS Trans. Power Electron. Applicat.*, vol. 1, no. 1, pp. 92–103, Dec. 2016.

[14] J. He, A. Sangwongwanich, Y. Yang, and F. Iannuzzo, "Lifetime evaluation of three-level inverters for 1500-V photovoltaic systems," *IEEE J. Emerg. Sel. Top. Power Electron.*, 2020, Early Access.

[15] Jinko. JKM380M-72-V solar panel. (2021). [Online]. Available: https://www.jinkosolar.com/uploads/5e68b53d/c4.pdf

[16] D. Sera, R. Teodorescu, and P. Rodriguez, "PV panel model based on datasheet values," in *Proc. IEEE ISIE*, pp. 2392–2396, 2007.

[17] J. Wiles, *Photovoltaic Power Systems for Inspectors, Plan Reviewers and PV Professionals: Based on the NEC 2017*. International Association of Electrical Inspectors, 2018.

[18] Semikron. IGBT Module MiniSKiiP II 3: SKiiP 39MLI12T4V1. (2021). [Online]. Available: https://www.semikron.com/products/product-classes/igbt-modules/detail/skiip-39mli12t4v1-25230510.html

[19] J. He, A. Sangwongwanich, Y. Yang, and F. Iannuzzo, "Thermal performance evaluation of 1500-VDC photovoltaic inverters under constant power generation operation," in *Proc. IEEE CPERE*, pp. 579–583, 2019.

[20] E. Serban, C. Pondiche, and M. Ordonez, "Modulation effects on power-loss and leakage current in three-phase solar inverters," *IEEE Trans. Energy Conversion*, vol. 34, no. 1, pp. 339–350, Mar. 2019.

[21] Semikron. Application manual – Power semiconductors. (2015). [Online]. Available: https://www.semikron.com

[22] X. Yuan, "Analytical averaged loss model of a three-level T-type converter," in *Proc. IET PEMD*, pp. 1–6, 2014.

[23] A. Sangwongwanich, Y. Yang, D. Sera, F. Blaabjerg, and D. Zhou, "On the impacts of PV array sizing on the inverter reliability and lifetime," *IEEE Trans. Ind. Appl.*, vol. 54, no. 4, pp. 3656–3667, 2018.

[24] L. F. N. Lourenço, M. B. de Camargo Salles, R. M. Monaro, and L. Quéval, "Technical cost of operating a photovoltaic installation as a STATCOM at nighttime," *IEEE Trans. Sustain. Energy*, vol. 10, no. 1, pp. 75–81, 2019.

[25] Y. Yang, H. Wang, F. Blaabjerg, and K. Ma, "Mission profile based multi-disciplinary analysis of power modules in single-phase transformerless photovoltaic inverters," in *Proc. EPE*, pp. 1–10, Sep. 2013.